ISSN: 2993-5326

Research Article

Journal of Applied Surface Science

Non-Destructive Characterization and Evaluation of Solid-State Battery In-Situ Solidification and Formation Processes Based on Ultrasonic Imaging Technology

Zhiguo Zhang[1], Haitao Li[2], Bowen Xiang[3], Fuchen Huang[4], Boran Xiang[5], Chun Peng[6] and Yong Xiang[1*]

[1]*Tsing Bosch (Zhuhai) Technology Co., Ltd, Zhuhai, China*

[2]*Beijing Products Quality Supervision and Inspection Research Institute, Beijing 101300, China*

[3]*University of Electronic Science and Technology of China, Zhongshan Institute*

[4]*School of International Education, Beijing University of Chemical Technology, Beijing, China*

[5]*Beijing Huijia Private School, Beijing, China*

[6]*Solid (Beijing) Technology Co., Ltd, Beijing, China*

[*]Corresponding Author
Yong Xiang, Tsing Bosch (Zhuhai) Technology Co., Ltd, Zhuhai, China.

Submitted: 2024, Dec 20; **Accepted:** 2025, Jan 27; **Published:** 2025, Feb 14

Citation: Xiang, Y., Zhang, Z., Li, H., Xiang, B., Huang, F., et al. (2025). Non-Destructive Characterization and Evaluation of Solid-State Battery In-Situ Solidification and Formation Processes Based on Ultrasonic Imaging Technology. *J Applied Surf Sci, 3*(1), 01-07.

Abstract

Solid-state batteries (SSBs) are poised to address energy demand challenges. Nonetheless, quality issues in SSBs manufacturing pose safety risks and degrade performance. This paper presents non-destructive characterization of the infiltration, in-situ solidification, and formation of SSBs for the first time via ultrasonic imaging technology (UIT) provides a new characterization method of SSBs and in-situ solidification degree and uniformity assessment. The results demonstrate that solid-state electrolyte precursor solution infiltrated SSBs exhibit strong ultrasonic wave transmission, which decreases significantly after the in-situ solidification process. This phenomenon is attributed to the volume shrinkage causing ultrasonic waves to be reflected. During the formation process, lithium deposition and electrode expansion occur, allowing ultrasonic waves to pass through the battery. This study is the first to delve into the propagation of ultrasonic waves within SSBs and it is anticipated that provide a theoretical foundation for the application of UIT in SSBs and guide manufacturing processes.

Keywords: Solid-State Batteries (SSBs), Ultrasonic Imaging, In-Situ Solidification, Formation

1. Introduction

By now, lithium-ion batteries (LIBs) have become indispensable in daily life. However, conventional liquid LIBs are unable to meet the increasing energy demands and face safety issues such as gassing and lithium plating, which require urgent solutions. Solid-state batteries (SSBs) are poised to address these challenges. Nonetheless, issues like incomplete infiltration, uneven in-situ solidification of solid-state electrolytes (SSEs) and incomplete degassing during processing pose significant safety risks to SSBs and severely degrade SSB performance. Effectively characterizing these issues could not only deepened insights into failure mechanisms and electrochemical behavior but also directed the refinement of manufacturing techniques.

In contrast to techniques that demand cell disassembly for the chemical measurement like XRD, SEM, EDS, and XPS, in-situ

techniques such as Gibbs free energy, EIS, AC impedance and OCV offer enhanced convenience while preserving the battery's pristine condition [1-4]. Nonetheless, the aforementioned techniques characterize the ensemble state of the battery through the reflection of electrical parameters and other physical metrics, which are indirect indicators and lacking ability of positioning battery abnormalities. Consequently, the use of in-situ imaging characterization represents an indispensable approach for detailed analysis. As a result, in-situ X-RAY CT, neutron imaging, in-situ SEM, model simulation and operando electron energy-loss spectroscopy have been advanced significantly [5-11]. Nevertheless, the high costs, low efficiency, and stringent requirements for characterization environments associated with these methods pose significant challenges to their integration into manufacturing protocols.

The application of ultrasonic imaging technology (UIT) allows for low-cost, in-situ, non-destructive characterization of lithium-ion batteries. In recent studies, researchers have adopted this technology to in-situ examine electrolyte wetting, gas evolution, and to refine parameters for efficient large-scale battery manufacturing. The evidence presented in the previous studies confirms that UIT has considerable potential for application in the field of LIBs research and manufacturing processes [12-13]. The in-situ solidification and formation stage of SSBs is accompanied by chemical reactions that induce mysterious physical transformations and ultrasonic wave is sensitive to the transformations. Therefore, UIT could provide essential visibility into the in-situ solidification process and formation kinetics of SSBs, significantly contributing to the refinement of production techniques and the deepening of our understanding of battery behavior. However, although researchers are actively exploring the application of UIT in SSBs, there is still no research on the characterization of the in-situ solidification and formation process in ultrasonic imaging. Additionally, the investigation into the alterations in acoustic impedance resulting from internal transformations during this process remains an understudied area [14].

Addressing this research gap, this paper employs UIT to characterize and visualize the in-situ solidification and formation process of SSBs. This study marks the first application of UIT to characterize the in-situ solidification and formation stages of SSBs. In-situ solidification degree and uniformity are subsequently assessed. Moreover, the theoretical interpretation of the evident variation in ultrasonic amplitude across the in-situ solidification and formation stages is expected to offer valuable insights into improving our understanding of these complex processes. With this anticipation, this paper aims to offer a research methodology for SSBs, providing a theoretical foundation for ultrasonic propagation within these batteries and guiding the optimal conditions for in-situ solidification and formation processes in practical manufacturing.

2. Fundamental Principle

2.1. Ultrasonic Imaging

The fundamental principle of ultrasonic imaging technology is the detection of varying degrees of attenuation of ultrasonic waves as they pass through materials with distinct acoustic impedances. This attenuation, along with the material's reflection and transmission characteristics, forms the basis for generating detailed images that reveal the internal structure and properties of the material. The passage of ultrasonic waves across the interface between two different media allows for the calculation of the transmission and reflection coefficients as following.

Transmission rate:$T=4Z_1 \cdot Z_2/(Z_1 + Z_2)^2$
Reflection rate: R=(Z2-Z1)^2/(Z1+Z2)2
Z_1, Z_2 are the acoustic impedances of the incident and emergent media.

The similarity of acoustic impedances Z1 and Z2 at the interface of two different media results in a higher transmission ratio, while a difference in acoustic impedances Z1 and Z2 leads to a higher reflection ratio. The acoustic impedance of gases is approximately 0.0004 MRayl, whereas the acoustic impedance of liquids and solids ranges from 1 to 50 MRayl. The vast difference in impedance indicates that ultrasonic waves may lose over 99.99% of their transmitted intensity at gas/solid interfaces. Consequently, the presence of even a small quantity of gas can substantially diminish the ultrasonic transmissibility.

2.2. SSBs Manufacturing Processes

On the other hand, during the formation of SSBs, due to the growth of SEI by electrochemical reactions and the generation of byproducts, the acoustic impedance of the acoustic medium is completely different. By tracking this change, the real-time characterization of the changes inside the battery during the formation process can be effectively achieved.

SSBs also have electrolyte infiltration steps while solution is different. By injecting a solid-state electrolyte precursor solution formed by low-viscosity monomers, initiators and lithium salts into the cell, a majority of pores in the electrode are filled with the precursor solution.

Following the infiltration of precursor solution, it undergoes in-situ solidification by in-situ polymerization reaction under the influence of the external environment. After the process of heating/photocuring and in-situ solidification, the precursor solution undergoes a transformation into a solid-state material, establishing a robust interface between the electrode and the electrolyte. The in-situ solidification process involves a transformation of the acoustic medium inside the battery from liquid to solid via cross-linking, an event that is inevitably accompanied by changes in the acoustic impedance of the material, thereby affecting the propagation of ultrasound. Through the comparison of ultrasonic signals prior to and subsequent to the in-situ solidification process, real-time characterization of the in-situ solidification process and the evaluation of the degree of in-situ solidification can be accomplished.

The process of SEI film formation in liquid lithium batteries is analogous to the reaction of solid electrolytes at the interface with

the electrode, resulting in the formation of a complex interfacial film. The high metallic activity of the lithium metal electrode in SSBs leads to electrochemical corrosion upon contact with the electrolyte, initiating the formation of a protective passivation layer. Throughout the formation of SSBs, the interfacial reaction continues under the influence of electrical current, resulting in lithium deposition at the interface. This gradually thickens the interface layer. As the electrical application duration and current density increase, lithium penetration phenomena occur. Lithium dendrites will fill the pores of the solid electrolyte.

3. Experimental

3.1. Sample

The batteries utilized in this experiment are self-assembled pouch batteries, specifically of the stacked type, comprising a total of 49 layers in the stack configuration. The cathode material is $Li_{3x}La_{2/3-x}TiO_3$ and anode material is metallic lithium. There are four battery samples, namely battery-1, battry-2, battery-3 and battery-4 respectively. The size of pouch batteries are 225mm*98mm, 225mm*135mm, 350mm*100mm and 350mm*100mm respectively. In the experimental procedure, ultrasonic images were captured using UIT at various stages for samples Battery-1, Battery-3, and Battery-4: infiltrated stage, after the in-situ solidification process, and the formation process. Additionally, for sample Battery-2, ultrasonic images were recorded infiltrated stage and after the in-situ solidification process.

3.2. Characterization Method

The ultrasonic characterization test equipment used in this experiment is independently developed by Tsing Bosch Co., Ltd., and the model number is Lithium Battery Safety Ultrasonic Testing Workstation Pro. The measurement setup presented as Figure.1. The coupling method of UIT is silicon oil coupling. The frequencies of ultrasonic probes are 1MHz which is independently developed by Tsing Bosch Co., Ltd. The focal distance of probes are 4 inch. Scanning speed is 100mm/s and step interval is 0.5mm which is same as resolution of ultrasonic image. The ultrasonic signal-gain is set at 15db.

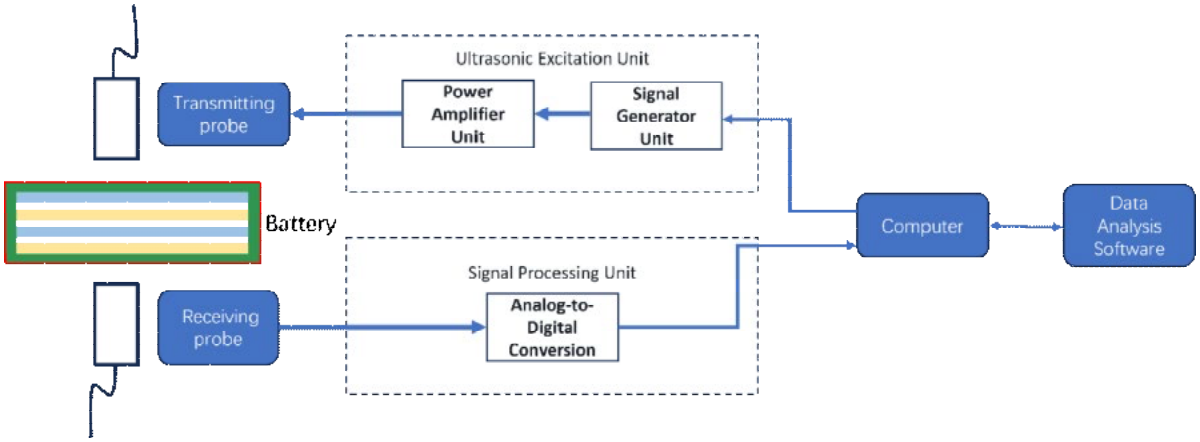

Figure 1: Measurement Setup

3.3. Infiltration and In-Situ Solidification Process

The electrolyte used in the experiment is LiFePO4 electrolyte purchased from CANRD Co., Ltd. The infiltration conditions are to maintain at -95.3 bar for 1.0 minute and -63.4 bar for 2.0 minutes, then return to atmospheric pressure, followed by another cycle. Finally, let batteries stand for 12 hours. The precursor is N, N'-Methylenebisacrylamide (MBA) and initiator is 2,2'-Azobis(2-methylpropionitrile) (AIBN). Both are purchased from Shanghai Aladdin Biochemical Technology Co., Ltd. The conditions for in-situ solidification of the battery are at a pressure of 0.7 MPa and a temperature of 50℃, maintained for 12 hours.

4. Result

4.1. Infiltrate Characterization

As shown in Figure.2, the ultrasonic imaging of the solid-state electrolyte precursor solution post-infiltration is visualized. In the upper right corner of Battery-1, an anomalous signal transmission phenomenon is detected. The surface of the battery pack indicates that the anomalous signal transmission is likely caused by a minor bulge. The transmission energy at the right side is found to be higher than that of the battery body, which is suspected to be due to precursor solution accumulation. Figure.2(b) illustrates Battery-2 with a characteristic blue ring area. Combined with process analysis, it is deduced that the blue ring area on Battery-2 is a discrete bubble resulting from incomplete degassing. The absence of transmission signals in the middle area of Battery-3 and Battery-4 is attributed to the short infiltration time.

The ultrasound imaging analysis reveals that during the infiltration stage, ultrasonic waves exhibit good transmission through the reagent, effectively characterizing the infiltration status within the battery. For the bubbles within the battery, the significant difference in acoustic impedance causes the ultrasonic signals to be reflected, resulting in the absence of transmission signals which could be basis for infiltration assessment.

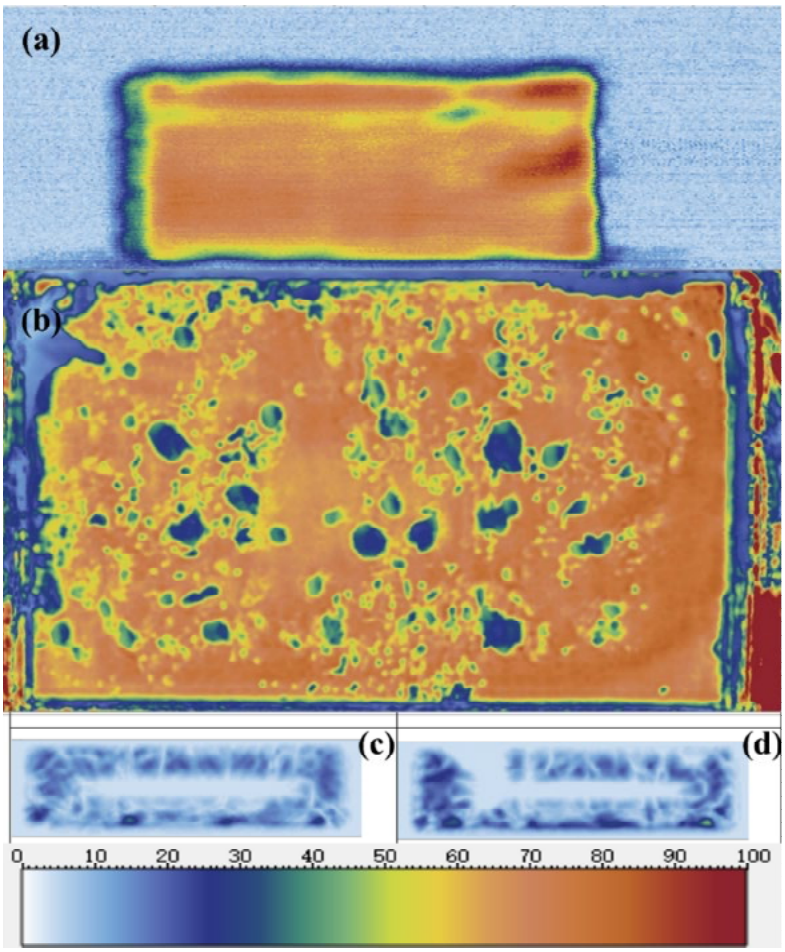

Figure 2: Ultrasonic Imaging of Infiltration of (a) Battery-1; (b) Battery-2; (c) and (d) Battery-3 and battery-4

4.2. Solidification Characterization

The ultrasonic imaging of the solid-state battery after in-situ solidification is shown in the figure.3. As depicted in Figure.3(a), in comparing the ultrasonic imaging during the infiltration stage, it is observed that the ultrasonic transmission signal is significantly diminished. The ultrasonic transmission waves are only detected in the middle region of the battery. This suggests that after the in-situ solidification process, the ultrasonic signal's ability to transmit is greatly reduced. An examination of the contrast between Figure.3(b) and Figure.3(c) shows that the ultrasonic signal's transmittance is markedly enhanced after increasing the excitation energy, and a broader spectrum of regions shows transmission signals. In Figure.3(d-f), Battery-2, Battery-3 and Battery-4 appear entirely blank, with no signals detected except for the edges of the batteries visible at the bottom of the images.

It is deduced from the aforementioned figures that SSBs following in-situ solidification do not display transmission signals, as opposed to the SSBs prior to infiltration

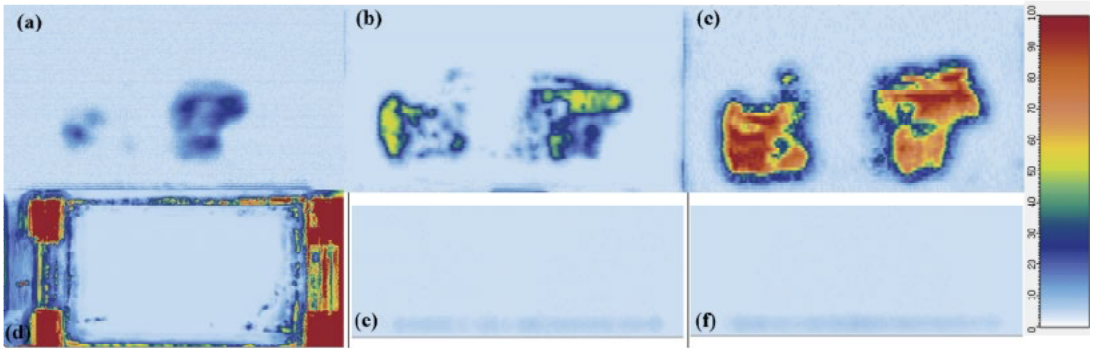

Figure 3: Ultrasonic Imaging of In-Situ Solidification of (a)Battery-1 under 15dB;(b) and (c) under 30dB and 40dB Gain Respectively; (d) Battery-2; (e) Battery-3 and battery-4

4.3. Formation Characterization

As shown in the Figure.4, the ultrasonic imaging images of the battery-1, battery-3 and battery-4 after formation process. It is observed that the ultrasonic transmission signal intensity of the SSBs after the formation process has significantly increased overall. The black framed area in Figure.4(a) has a low amplitude due to the bulging of battery bubbles after formation, which is consistent with the appearance characteristics of the battery. The red frame shows a low-transmission wave area in an independent circular area. The occurrence of gas production inside the battery is confirmed by inspecting the external appearance of the battery. Additionally, a linear area in black framed of the battery shows no ultrasonic transmission signal due to imaging limitations of the equipment.

It can be seen from the above figure, the ultrasonic signal transmittance of SSBs after formation is greatly increased compared with the cured battery.

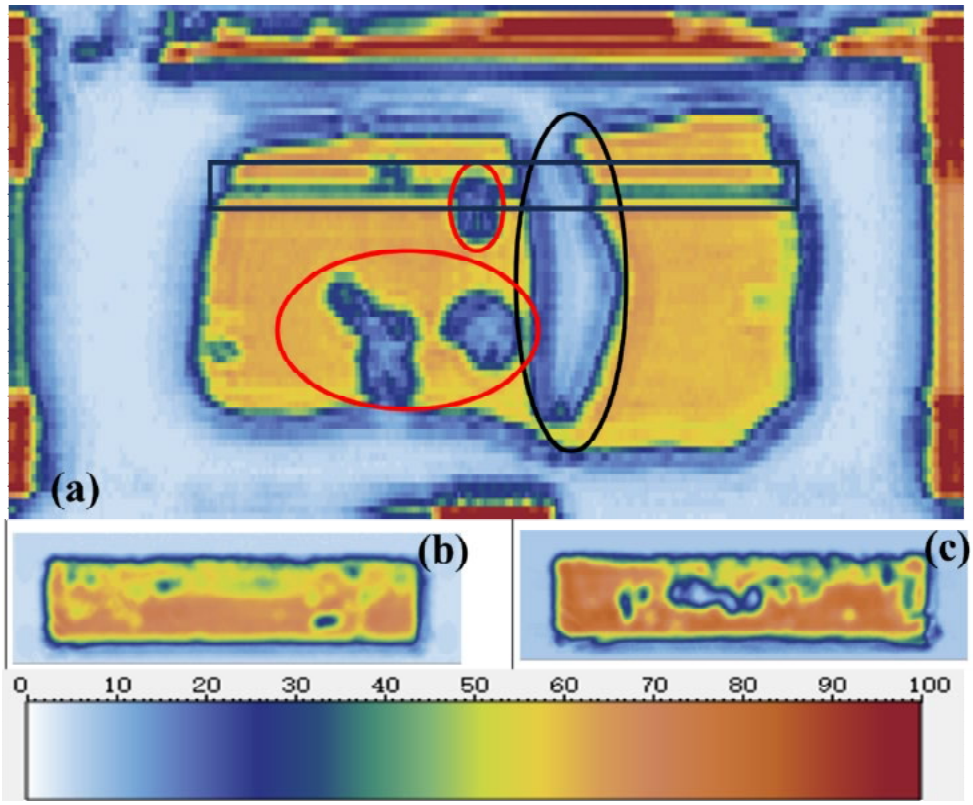

Figure 4: Ultrasonic Imaging of Formation of (a) Battery-1; (b) and (c) Battery-3 and battery-4

5. Explanation and Assessment

5.1. In-Situ Solidification Process

During the in-situ solidification process, the contraction of the solid electrolyte is an unavoidable occurrence. The van der Waals force polymerizes monomers becomes a covalent bond force. The covalent bond force is significantly stronger, leading to a reduction in the distance between molecules. The observable effect of the increased covalent bond force is a decrease in volume, leading to volume shrinkage [15]. Prior to the gel point of the in-situ polymerization reaction, the monomer can alleviate volume shrinkage through self-flowing, and no shrinkage stress is induced at this time. Once the gel point is reached, the monomer solidifies and cannot flow, thus unable to compensate for volume shrinkage, resulting in shrinkage stress [16]. In addition, the cross-linking reaction of the polymer is also an important factor. During the in-situ solidification process, the polymer chains form a network structure through chemical bonds, which leads to volume shrinkage. From the perspective of surface energy, the evaporation of liquid from the gel results in the formation of a new solid/gas interface at the original solid/liquid interface. The solid/gas interface possesses a higher energy than the solid/liquid interface, leading to an increase in the system's energy. This increased energy causes the liquid to migrate from the interior to the exterior of the system. During this process, the liquid is subjected to tensile stress, which exerts compressive force on the skeleton, resulting in its compression and shrinkage.

This shrinkage phenomenon usually starts from the middle area of the solid electrolyte and then gradually spreads to the edge, forming a concave shape. The reason for the shrinkage from the middle area is usually related to the evaporation of the solvent and the cross-linking process of the polymer. During the in-situ solidification process, the solvent evaporates. As the middle area of the material is closer to the heat source or reaction area than the edge area, the solvent evaporates more rapidly, leading to volume contraction in the middle area before the edge. Since the

middle area of the material may reach the threshold of the cross-linking reaction earlier than the edge area, the middle area begins to shrink first. The volume shrinkage displacement in the vertical direction of the in-situ solidification can reach 0.300mm, and this shrinkage displacement can reach 0.025mm in the edge area of the solid electrolyte [17]. This will cause a cavity to appear between the electrode and the solid electrolyte. The in-situ polymerization reaction and cross-linking reaction during the in-situ solidification process will generate gases, which will remain in the cavity [18-19]. The ultrasonic wave has a large attenuation in the cavity, so the transmission wave is reflected in the solid-state battery, resulting in a blank in transmission signal. On the other hand, since the in-situ solidified solid electrolyte has a large porosity and cracking will occur around the solid electrolyte due to the stress change caused by shrinkage, filling gas may also cause the attenuation of the ultrasonic signal.

The presence of this gap can lead to a poor contact between the electrode. As part of the manufacturing process, strategies such as adding fillers or enhancing the effectiveness of binders are commonly employed to address volume shrinkage and improve contact performance. When the gap between electrolyte and electrode is small, a subset of ultrasonic waves is still able to transmit. This is the explanation for the presence of ultrasonic transmission signals observed in Figure.3(a)-(c) with enhanced signal-gain.

Therefore, during the in-situ solidification stage, the degree of attenuation of the ultrasonic signal represents the degree of in-situ solidification. As shown in Figure.3 (a-c), a large area of ultrasonic signals appeared in Battery-1, indicating a lower degree of solidification and non-uniform solidification which could potentially affect its performance and reliability. In Battery-2, there are still areas where ultrasonic signals are present, indicating non-uniform solidification in these regions. This suggests that the in-situ solidification process may not have been uniform across the entire battery. The statement that Battery-3 and Battery-4 have uniform in-situ solidification suggests that the in-situ solidification process for these batteries was more controlled and effective compared to Battery-1 and Battery-2.

5.2. Formation Process

During the formation process, under the action of current, the internal volume of the solid-state battery will change. This is because during the charge and discharge process, lithium ions are inserted and de-inserted. In the LTO solid-state battery, the volume change of the entire battery is dominated by the lithium metal negative electrode [20]. Therefore, in the solid-state battery, the volume expansion is mainly caused by the lithium metal negative electrode. The expansion is attributed to reduce the gas gap. Moreover, during the formation process, the increase in current density will promote the deposition of lithium on the surface of the lithium metal negative electrode, resulting in the thickening of the lithium deposition layer [21]. This is also an important reason for the volume expansion during the charge and discharge process of the solid-state battery.

Another important reason is the deposition of lithium inside the lithium metal negative electrode during the charge and discharge process. The study shows that the lithium deposition thickness of the Li/LLZTO/Li battery measured at a current density of 1, 2, and 3 mA/cm2 is 12, 24.5, and 38 μm, accompanied by a negative electrode volume expansion rate of 145-158% [22]. Lithium deposition and volume expansion can effectively fill the cavity between the electrode during the in-situ solidification process and expel the gas, so that the ultrasonic signal can be transmitted. At the same time, under the action of current density, lithium penetration will occur. Lithium will tend to grow towards the defects and pores of the solid electrolyte [23-24]. This lithium penetration phenomenon will fill almost all the gaps between LLZTO particles, which can effectively discharge gas and reduce the attenuation of ultrasonic transmission signals [22].

As demonstrated above, the electrode expansion, lithium deposition, and lithium penetration serve to reduce and complete the gap, releasing gas internally. This allows the ultrasonic transmission signal to transmit through and be detected. Therefore, UIT can be used to assess the volume expansion, lithium deposition, and gas evolution during the forming stage of SSBs.

6. Conclusion

In this paper, we employ ultrasonic imaging equipment developed by Tsing Bosch Co., Ltd., to characterize SSBs infiltration, in-situ solidification and formation process. The results demonstrate that infiltrated SSBs display strong ultrasonic wave transmission. Upon completion of the in-situ solidification process, ultrasonic transmission signals experience a marked decrease, which is restored to a high level upon the completion of the formation process. The elucidation of this phenomenon is offered in this paper. In infiltrated SSBs, the solvents have a high acoustic impedance, which facilitates the transmission of ultrasonic waves. Following in-situ solidification, the volume shrinkage resulting from in-situ polymerization reaction creates a gas layer between electrolyte and solid-state electrolyte with low acoustic impedance. Consequently, ultrasonic waves are reflected, leading to the absence of transmission signals. During the formation process, lithium deposition and electrode expansion occur, filling the gaps. As a result, ultrasonic waves can once again pass through the battery. Based on this, UIT can achieve non-destructive testing of the degree of in-situ solidification, uniformity, as well as volume expansion after forming, lithium deposition thickness, and gas evolution. This paper presents a comprehensive characterization of the infiltration, in-situ solidification, and formation processes of SSBs for the first time via ultrasonic imaging system developed by Tsing Bosch Co., Ltd., provides a new characterization method of solid-state battery and in-situ solidification degree and uniformity assessment. It is anticipated that this paper will lay a theoretical foundation for the application of ultrasonic imaging technology in SSBs and provide guidance for manufacturing processes.

Reference

1. Jin, D., Kang, H., Do, H. W., Kim, G., Kim, T., Kim, S., ... & Shim, W. (2021). Enhancing li ion battery performance by

mechanical resonance. *Nano letters, 21*(12), 5345-5352.
2. Günter, F. J., Burgstaller, C., Konwitschny, F., & Reinhart, G. (2019). Influence of the electrolyte quantity on lithium-ion cells. *Journal of The Electrochemical Society, 166*(10), A1709-A1714.
3. Wu, M. S., Liao, T. L., Wang, Y. Y., & Wan, C. C. (2004). Assessment of the wettability of porous electrodes for lithium-ion batteries. *Journal of applied electrochemistry, 34*, 797-805.
4. Cui, H., Ren, D., Yi, M., Hou, S., Yang, K., Liang, H., ... & He, X. (2022). Operando monitoring of the open circuit voltage during electrolyte filling ensures high performance of lithium-ion batteries. *Nano Energy, 104*, 107874.
5. Schilling, A., Gümbel, P., Möller, M., Kalkan, F., Dietrich, F., & Dröder, K. (2018). X-ray based visualization of the electrolyte filling process of lithium ion batteries. *Journal of The Electrochemical Society, 166*(3), A5163.
6. Hagemeister, J., Stock, S., Linke, M., Fischer, M., Drees, R., Kurrat, M., & Daub, R. (2023). Lean Cell Finalization in Lithium-Ion Battery Production: Determining the Required Electrolyte Wetting Degree to Begin the Formation. *Energy Technology, 11*(5), 2200686.
7. Chen, H. S., Yang, S., Song, W. L., Yang, L., Guo, X., Yang, X. G., ... & Fang, D. (2023). Quantificational 4D visualization and mechanism analysis of inhomogeneous electrolyte wetting. Etransportation, 16, 100232.
8. Günter, F. J., Rössler, S., Schulz, M., Braunwarth, W., Gilles, R., & Reinhart, G. (2020). Influence of the cell format on the electrolyte filling process of lithium-ion cells. *Energy Technology, 8*(2), 1801108.
9. Sagane, F., Shimokawa, R., Sano, H., Sakaebe, H., & Iriyama, Y. (2013). In-situ scanning electron microscopy observations of Li plating and stripping reactions at the lithium phosphorus oxynitride glass electrolyte/Cu interface. *Journal of power sources, 225*, 245-250.
10. Li, Q., Yi, T., Wang, X., Pan, H., Quan, B., Liang, T., ... & Li, H. (2019). In-situ visualization of lithium plating in all-solid-state lithium-metal battery. *Nano Energy, 63*, 103895.
11. Nomura, Y., Yamamoto, K., Fujii, M., Hirayama, T., Igaki, E., & Saitoh, K. (2020). Dynamic imaging of lithium in solid-state batteries by operando electron energy-loss spectroscopy with sparse coding. *Nature communications, 11*(1), 2824.
12. Deng, Z., Huang, Z., Shen, Y., Huang, Y., Ding, H., Luscombe, A., ... & Dahn, J. R. (2020). Ultrasonic scanning to observe wetting and "unwetting" in Li-ion pouch cells. *Joule, 4*(9), 2017-2029.
13. Hou, S., Yi, M., Jiang, F., Lu, L., Ren, J., Fuhrmann, M., ... & Lai, X. (2023). Ultrasonic testing-based method for segmental calibration and quantitative estimation of the electrolyte content in lithium-ion batteries. *Measurement, 217*, 113101.
14. Huo, H., Huang, K., Luo, W., Meng, J., Zhou, L., Deng, Z., ... & Huang, Y. (2022). Evaluating interfacial stability in solid-state pouch cells via ultrasonic imaging. *ACS Energy Letters, 7*(2), 650-658.
15. Dewaele, M., Truffier-Boutry, D., Devaux, J., & Leloup, G. (2006). Volume contraction in photocured dental resins: the shrinkage-conversion relationship revisited. *Dental Materials, 22*(4), 359-365.
16. Giachetti, L., Bertini, F., & Bambi, C. (2007). A rational use of dental materials in posterior direct resin restorations in order to control polymerization shrinkage stress. *Minerva stomatologica, 56*(3), 129-138.
17. Yang, H., Wang, A., Xia, H., Wang, S., Liu, J., Ao, X., ... & Shi, J. (2023). Inverse identification of in-situ curing shrinkage using a method combining 3D digital image correlation and finite-element simulation. *Measurement, 223*, 113760.
18. Zhang, S., Xie, B., Zhuang, X., Wang, S., Qiao, L., Dong, S., ... & Cui, G. (2024). Great challenges and new paradigm of the in situ polymerization technology inside lithium batteries. *Advanced Functional Materials, 34*(17), 2314063.
19. Liu, Q., Wang, L., & He, X. (2023). Toward practical solid-state polymer lithium batteries by in situ polymerization process: a review. *Advanced Energy Materials, 13*(30), 2300798.
20. Gu, J., Chen, X., He, Z., Liang, Z., Lin, Y., Shi, J., & Yang, Y. (2023). Decoding Internal Stress-Induced Micro-Short Circuit Events in Sulfide-Based All-Solid-State Li-Metal Batteries via Operando Pressure Measurements. *Advanced Energy Materials, 13*(47), 2302643.
21. Swamy, T., Porz, L., Sheldon, B. W., Rettenwander, D., Frömling, T., Thaman, H., ... & Chiang, Y. M. (2017, September). Mechanism of Lithium Metal Penetration through Inorganic Solid Electrolytes. In *Electrochemical Society Meeting Abstracts 232* (No. 4, pp. 423-423). The Electrochemical Society, Inc.
22. Zhu, J., Li, X., Wu, C., Gao, J., Xu, H., Li, Y., ... & Zhou, W. (2021). A multilayer ceramic electrolyte for all-solid-state Li batteries. *Angewandte Chemie International Edition, 60*(7), 3781-3790.
23. Ren, Y., Shen, Y., Lin, Y., & Nan, C. W. (2015). Direct observation of lithium dendrites inside garnet-type lithium-ion solid electrolyte. *Electrochemistry Communications, 57*, 27-30.
24. Yan, K., Lu, Z., Lee, H. W., Xiong, F., Hsu, P. C., Li, Y., ... & Cui, Y. (2016). Selective deposition and stable encapsulation of lithium through heterogeneous seeded growth. *Nature Energy, 1*(3), 1-8.